Catalysis Letters, Vol. 116, Nos. 3–4, August 2007 (© 2007)
DOI: 10.1007/s10562-007-9125-6

Direct observation of carbon nanotube formation in Pd/H-ZSM-5 and MoO_3/H-ZSM-5 based methane activation catalysts

S. Burns,[a] J. G. Gallagher,[a] J. S. J. Hargreaves,[a,]* and P. J. F. Harris[b]

[a]*WestCHEM, Department of Chemistry, University of Glasgow, Joseph Black Building, Glasgow G12 8QQ, UK*
[b]*Centre for Advanced Microscopy, J. J. Thomson Physical Laboratory, University of Reading, Whiteknights, Reading RG6 6AF, UK*

Received 19 March 2007; accepted 12 April 2007

The nature of carbonaceous species deposited upon MoO_3/H-ZSM-5 and Pd/H-ZSM-5 based catalysts during methane activation at 700 °C has been studied. TEM evidences the formation of open-ended multi-walled carbon nanotubes on MoO_3/H-ZSM-5 based dehydroaromatisation catalysts. Pd/H-ZSM-5 is more active, exclusively towards methane cracking and post-reaction analysis reveals the distribution of different carbonaceous species is more homogeneous which TEM demonstrates to be in the form of closed-end multi-walled carbon nanotubes.

KEY WORDS: carbon nanotubes; methane; dehydroaromatisation; zeolite; TEM; TGA.

1. Introduction

In recent years the production of benzene by dehydroaromatisation has been the subject of much interest [1,2]. The most well studied catalytic system has been that based upon ZSM-5 supported MoO_3. In this system, it has been proposed that in the active state molybdenum is in the form of molybdenum carbide or molybdenum oxycarbide [2–5]. The reaction mechanism is generally considered to occur via the bifunctional activation of methane on the molybdenum containing phase with cyclisation being promoted by the Bronsted acid sites on the zeolite. It is often proposed that ethylene is the primary product of reaction, which is then cyclised to form benzene [6]. However, alternative proposals suggest the occurrence of acetylene as an intermediate [7], or indeed the involvement of partially dehydrogenated C_1 entities [8]. C_2 hydrocarbons, particularly ethylene, are reported to be co-products of the reaction and a distribution of aromatic products is observed. Whilst benzene is the major aromatic product, significant selectivities to other aromatic products such as naphthalene, methylnaphthalenes and toluene are frequently reported, e.g. [8,9]. In terms of the reaction mechanism, the latter two products comprising molecules with an odd number of carbon atoms, 11 and 7, respectively, demonstrate that the reaction cannot simply be considered in terms of exclusive cyclisation of C_2 intermediates.

The reaction is equilibrium limited and is generally run at 700 °C or above. Major obstacles to its application are low activity and limited lifetime. To date, the activity of the best catalysts is such that conversion approaching equilibrium is only achieved when low space velocities (typically 1000 h^{-1}) are applied. It is common that MoO_3 based catalysts will display an induction period, wherein the active phase is formed, which is followed by slow deactivation, frequently ascribed to the deposition of site blocking carbonaceous species, although some of the latter may be important for the development of activity. Within the literature, a number of strategies have been reported to increase activity and/or extend lifetime.

Ichikawa and co-workers first described the promotion of catalytic activity by the addition of Fe^{3+} or Co^{2+} dopants in terms of enhancement of both activity and retardation of deactivation [8,10]. Fe^{3+} was proposed to exert an influence by the reduction of the level of coke produced. The same group have also argued that the observed beneficial effects of the addition of low levels of CO to the reaction feedstream is via modification of the carbonaceous residues formed on the catalyst [9]. Elsewhere, in studies investigating MoO_3/MCM-22, proposals have been made that carbonaceous deposits are the primary product of reaction and that some forms of them can be directly hydrogenated to form C_2H_4 and C_6H_6 whereas other forms retard catalytic activity [11]. Within the literature, there have been many studies aimed at the elucidation of the nature of different carbon species. Such studies have generally taken the form of spectroscopic characterisation and/or the determination of reactivity of various forms of carbon using temperature programmed techniques. Attempts of direct observation of the forms of post-reaction carbon by, for

---

*To whom correspondence should be addressed.
E-mail: justinh@chem.gla.ac.uk

example, TEM appear to be somewhat limited. One such study has been directed towards a non-conventionally prepared catalyst where microwave heating has been applied to modify the dispersion of MoO_3 selectively on the external surface of the ZSM-5 host [12]. Based upon XPS evidence, Lunsford and co-workers have reported the formation of three types of carbon – adventitious or graphitic like carbon which has a binding energy of 284.6 eV and is mainly present in the zeolite channel system, carbidic type carbon in Mo_2C with a binding energy of 282.7 eV which is predominantly located on the external surface of the zeolite and a hydrogen poor sp-type or pre-graphitic carbon which covers both the zeolite surface and the Mo_2C phase [13]. It is the latter type of carbon which was proposed to cause deactivation. In cross-polarisation ^{13}C MAS NMR spectroscopy studies on spent catalysts, Jiang *et al.* [14] distinguished two forms of carbonaceous residue, one associated with acid sites of the zeolite and the other associated with molybdenum species. There have been many studies employing temperature programmed techniques. For example, Xu and co-workers have reported that two different types of carbonaceous species are formed on post-reaction catalyst [15]. By employing a combination of TGA, TPO, TPR and temperature programmed reaction with CO_2, the differing reactivities of such species were probed. So-called low temperature species (i.e. those which are removed at the lower temperature by TPO or TGA in air) are generally ascribed to carbonaceous species associated with carbonaceous species associated with the molybdenum phase, whereas high temperature species are associated with the zeolite Bronsted acid sites.

Coke deposition has also been reported to be problematic in other non-molybdenum containing systems. For example, Weckhuysen *et al.* [16] have demonstrated the activity of pre-reduced Fe_2O_3/ZSM-5. XPS demonstrated that neither metallic iron nor iron carbide was formed. However, deleterious coke deposition related to a C 1s signal at 283.5 eV was proposed to decrease selectivity to aromatics with time on stream.

In the present study, we have made a TGA based study on the reactivity of post-reaction carbon in various MoO_3/H-ZSM-5 catalysts and have sought to make direct observation of the nature of such carbon by TEM. Furthermore, a comparison of the catalytic activity and of MoO_3/H-ZSM-5 and Pd/H-ZSM-5 is presented and the comparison of the post-reaction forms of carbon present on catalysts has been made.

2. Experimental

MoO_3/H-ZSM-5 based catalysts were prepared by impregnation of an aqueous solution of ammonium heptamolybdate onto H-ZSM-5 (Catal, Si/Al = 40) followed by drying and calcination as described previously [17]. The loading of MoO_3 applied was 3 wt%. Dopants were impregnated onto the calcined MoO_3/H-ZSM-5 from aqueous solutions of their nitrates so as to yield a dopant ion/Mo atomic ratio of 0.25, which corresponds to the region reported by Ichikawa and co-workers for optimum Fe^{3+} promotion [8]. Pd/H-ZSM-5 was prepared by a similar method in which an aqueous solution of palladium nitrate (Aldrich,$Pd(NO_3)_2 \cdot XH_2O$) was impregnated onto the same parent zeolite. The sample was then dried at 80 °C for 24 h prior to calcination in air at 500 °C for a further 16 h. The quantity of palladium nitrate impregnated corresponded to that required to yield a 3 wt% Pd loading.

CHN analysis was performed by combustion using a CE-440 elemental analyser. TGA was performed on a TA Instruments TGA Q500 series instrument. The catalyst charge was typically 0.02 g and the flowrate of air used was 90 ml min^{-1}. Catalysts were heated from room temperature to 900 °C in an air stream employing a ramp rate of 5 °C min^{-1}.

TEM analysis was performed using either an FEI Tecnai $G^2$20 T20 instrument (at University of Glasgow) or a JEOL 2010FX instrument (at University of Reading). Samples were dispersed in iso-propanol prior to deposition on lacey carbon support films.

Microreactor testing has been described in detail elsewhere [17,18]. In summary, catalysts were used in the form of powders held centrally within the heated zone of a quartz microreactor and were tested over a 6.5-h period. The feed gas composition applied was 80% CH_4 (BOC, 99.5%) and 20% N_2 (BOC 99.98%) which were flowed at a total rate of 10 ml min^{-1}, typically giving a GHSV of ca. 960 h^{-1}. Product analysis was performed by on-line gc (for H_2 and hydrocarbon quantification) and periodic FTIR analysis of exit stream composition in a flow cell (for quantification of CO and CO_2).

3. Results and discussion

In view of the widespread interest aimed at the elucidation of the nature of carbon containing residues in MoO_3/H-ZSM-5 based methane dehydroaromatisation catalysts as detailed in the introduction, it is perhaps surprising that relatively little effort has been directed towards their direct observation by TEM. In this manuscript, we describe our efforts to address this, having performed TEM analysis on MoO_3/ZSM-5 catalysts, and its counterpart doped with low a low level of Fe^{3+}, following reaction with methane at 700 °C for 6.5 h time on stream. The activities of such catalysts have been described in detail elsewhere [17]. In agreement with Ichikawa and co-workers, we observe that the inclusion of a low level of Fe^{3+} dopant has a beneficial effect on dehyrdoaromatisation activity, although in our studies we evidence an enhancement in the levels of carbon deposited in post-reaction samples, compared with the

MoO_3/ZSM-5 parent. The results of CHN combustion analysis are reported in table 1. The "corrected carbon value" quoted provides an indication of the non-carbidic carbon content of catalysts and is calculated by subtraction of the quantity of carbon corresponding to complete conversion of a 3 wt% loading of MoO_3 to Mo_2C. We [17], and others [19], have also observed that Ga^{3+} doping is beneficial to catalytic activity. As reported in table 1, like others, we observe that it reduces the overall level of coke produced with respect to the parent MoO_3/H-ZSM-5 catalyst.

In order to more fully characterise the nature of the coke formation in post-reaction catalysts, TGA studies in the presence of air have been undertaken and the first derivative profile for the post-reaction MoO_3/H-ZSM-5 parent catalyst is reported in figure 1. The general form of the profile is similar to those reported elsewhere [15,20]. The loss of water occurs below 150 °C and the combustion of carbonaceous species, which shows good agreement with the CHN analysis, occurs over a relatively large temperature range (ca. 420–650 °C). As is evident from the figure, the TGA peak profile for the loss of carbon by combustion can be fitted to at least two general peaks with maxima at ca. 460 and 590 °C. Within the literature, the lower temperature peak has been attributed to loss of carbon associated with the molybdenum carbide phase and that at higher temperature to carbon associated with carbon associated with zeolite phase, e.g. [15,20]. Also presented in figure 1, is derivative data for both the iron and gallium doped catalysts. Both dopants are observed to have a significant influence on the profile. It is interesting to note that the effect of gallium is to significantly reduce the higher temperature form(s) of the carbon whilst iron dramatically enhances its relative concentration and shifts the peak maximum downwards by ca. 15 °C. Given that both iron and gallium exhibit promotional effects, the data demonstrate that their promotional effects cannot be simply ascribed to a general effect on the carbonaceous deposits.

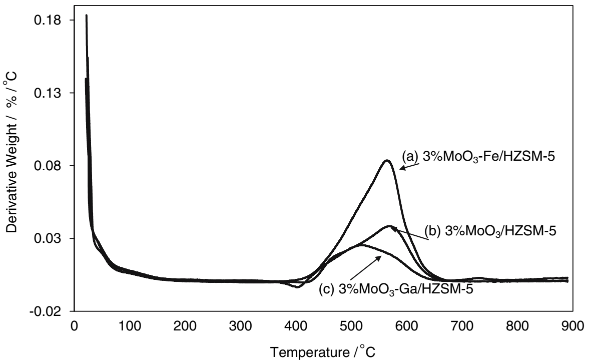

Figure 1. First derivative TGA pattern of post-reaction 3 wt% MoO_3/H-ZSM-5 and Fe^{3+} and Ga^{3+} doped counterparts following 6.5 h on stream.

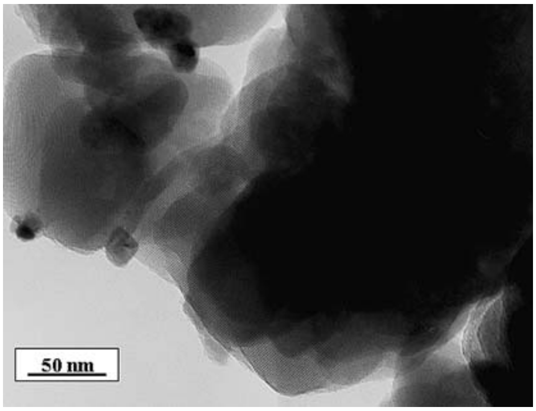

Figure 2. TEM of post-reaction 3 wt% MoO_3/H-ZSM-5 following 6.5 h on stream.

The results of TEM analysis of post-reaction MoO_3/H-ZSM-5 and Fe^{3+}–MoO_3/H-ZSM-5 catalysts are shown in figures 2 and 3. Both catalysts show similar general features with an in-homogeneous distribution of carbon. The micrographs presented are representative of both Fe^{3+} doped and undoped samples. As shown in figure 2 which relates to post-reaction MoO_3/H-ZSM-5, there are regions where very little carbon is evident, although large metallic like particles are dispersed on the external ZSM-5 surfaces. It is probable that these relate to the low dispersion of Mo_2C external surface crystallites as reported by Lunsford and co-workers [13]. Elsewhere, some regions can be found where there are extensive arrays of carbon nanotubes as shown in the micrograph of post-reaction Fe^{3+}–MoO_3/H-ZSM-5 in figure 3. To our knowledge the occurrence of carbon nanotube structures in post-reaction catalysts does not seem to have been widely recognised, although there is a report of their occurrence in non-conventionally prepared catalysts where a microwave technique has been applied to ensure distribution of MoO_3 on the external surface of ZSM-5 [12]. The nanotubes observed in our study have been found to be of multi-wall type. As can be seen in figure 3, there is a relatively large distribution in their diameter (in the range ca. 50–500 Å) and a number of tubes show kinks. Close analysis does not evidence the formation herring bone type structures. Figure 4 evidences the growth of such nanotubes in the

Table 1
CHN analysis of various post-reaction catalysts following 6.5 h time on stream

Catalyst precursor	C (wt%)	H (wt%)	N (wt%)	Corrected carbon value (wt%)
MoO_3/H-ZSM-5	4.21	0.14	–	4.08
Fe^{3+}–MoO_3/H-ZSM-5	5.69	0.15	–	5.56
Ga^{3+}–MoO_3/H-ZSM-5	3.09	–	–	2.96
Pd/H-ZSM-5	30.24	ND	ND	NA

ND = Not determined; NA = not applicable.

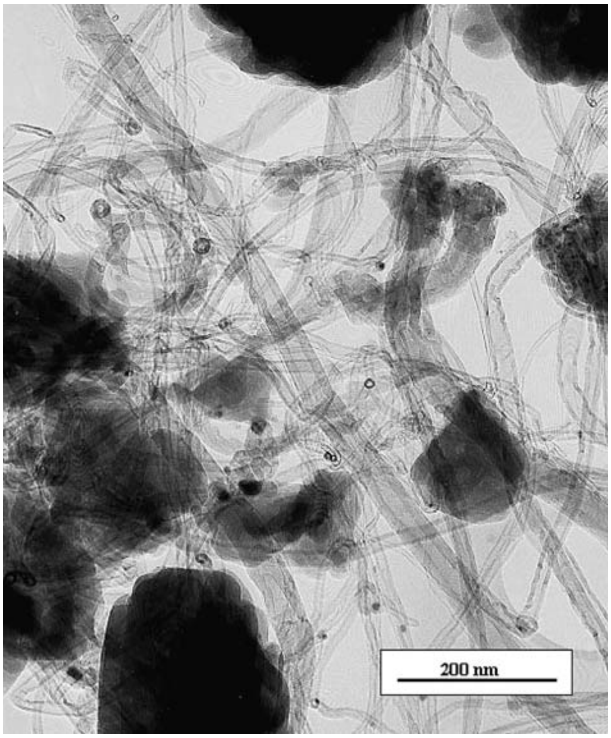

Figure 3. TEM of post-reaction Fe^{3+}–MoO_3/H-ZSM-5 following 6.5 h on stream showing a region with a high density of carbon nanotubes.

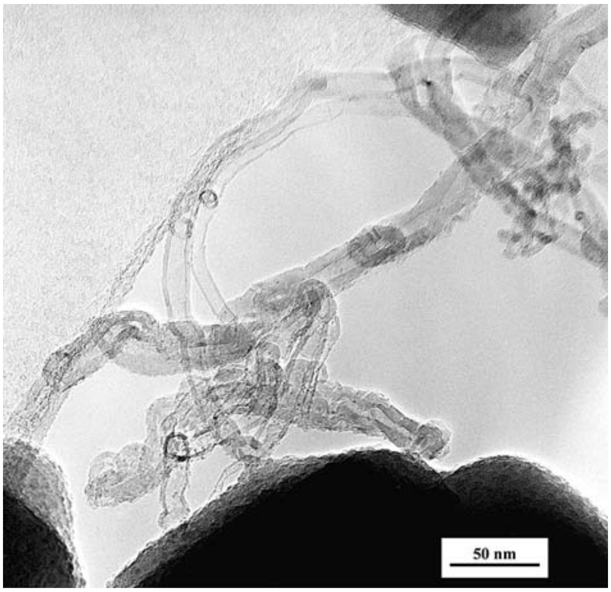

Figure 4. TEM of post-reaction Al^{3+}–MoO_3/H-ZSM-5 following 6.5 h on stream showing a region with the surface attachment on nanotubes to the ZSM-5 matrix, similar features are seen in other MoO_3/ZSM-5 based catalysts.

vicinity of the ZSM-5 crystallite for Al^{3+} doped MoO_3/H-ZSM-5. It is apparent that the nanotubes emanate from the external surface of the ZSM-5 crystallites and are not specifically associated with any localised structural damage to the zeolite or indeed with any large external particles. In addition, as can be seen, the nanotubes are open-ended and the absence of capping is indicative of a base growth mechanism. Deposits of disordered forms of carbon were also evidenced on all post-reaction catalysts.

In view of the widespread suggestion that the active form of the molybdenum species in the reaction is Mo_2C-like, we thought it of interest to make a comparison between the catalytic performance of MoO_3/H-ZSM-5 and Pd/H-ZSM-5. The basis for such a comparison is the widely reported similarity of catalytic behaviour between bulk phase molybdenum carbide and platinum group metals [21,22]. Accordingly, a 3 wt% Pd/H-ZSM-5 catalyst was prepared by aqueous impregnation as detailed in the experimental section. Following calcination, as for the MoO_3/H-ZSM-5 catalyst precursors, powder diffraction studies only evidenced reflections of the ZSM-5 framework which is indicative of the high dispersion and/or low concentration of the palladium component. Upon reaction, the catalyst was only observed to produce hydrogen, with no hydrocarbon products such as benzene being produced. Indeed the rate of hydrogen production was significantly higher than that for MoO_3/H-ZSM-5 under comparable conditions, as shown in figure 5. Unlike the MoO_3 containing catalyst, which shows a pronounced activation profile followed by a slow decline in activity over the period tested, the Pd based catalyst demonstrated an initial very high activity. Such differences in the performance of the two systems demonstrate that the Pd and MoO_3 derived components cannot be considered as analogous in behaviour. Whether this is as a consequence of, for example, the involvement of molybdenum oxycarbide species in the catalytic reaction, as proposed by some (e.g. [5]) , or represents a more general limitation in the comparative behaviour of molybdenum carbide or platinum group metals is not currently clear. The direct cracking of methane to produce C and H_2 is an area of intense current interest and represents a route to CO free H_2 which can find application both for PEM fuel cells and as a chemical feedstock [23].

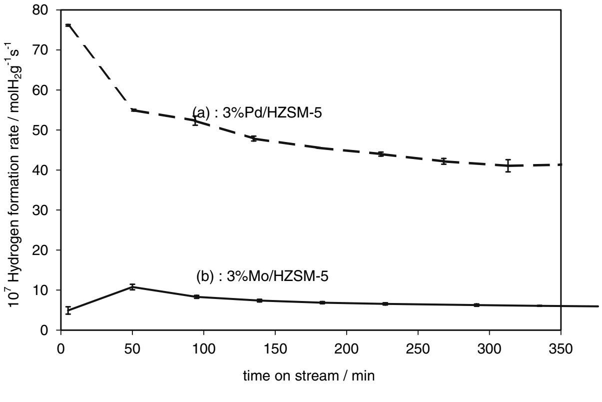

Figure 5. Comparative rates of H_2 formation for 3 wt% MoO_3/H-ZSM-5 and catalysts.

As expected, as shown in table 1, post-reaction CHN analysis showed that there is a significantly higher concentration of carbon in the post-reaction Pd/H-ZSM-5 catalyst. Post-reaction TGA studies showed the loss of carbon to occur over a much narrower temperature window (590–640 °C) than the MoO_3/H-ZSM-5 based counterparts, indicating that the form of carbon on this catalyst is much less heterogeneous. In TEM studies reported in figure 6, extensive formation of multi-walled carbon nanotubes is evidenced. Furthermore, upon close inspection, a number of these nanotubes are found to be defective, exhibiting a herring bone structure as shown in figure 6, unlike the MoO_3/ZSM-5 systems. The nanotubes formed within this system appear to be enclosed, but no evidence for metal crystallite capping was found, again suggesting the occurrence of a base growth mechanism. Within the carbon nanotube literature, a very recent report of nanotube formation on plasma and hydrogen pre-reduced Pd/H-ZSM-5 catalysts has been reported, although in that study micrographs demonstrating the capping of nanotubes by Pd crystallites was presented [24]. Our current studies are indicative that the pre-reduction of palladium precursors species is not a necessary requirement for nanotube formation in this system. Furthermore, despite high sensitivity for their detection, we did not observe the formation of CO or CO_2 in the exit gas-stream during reaction which indicates that reduction is rapid in relation to the sampling time.

The comparison between the behaviour of the MoO_3 and Pd based catalysts is worthy of note. In studies of hydrogen transfer reactions where similarities between the performance of molybdenum carbide phases and platinum group metals have been drawn, it is often observed that the activity of the carbide is lower. The observation of the formation of nanotubes, and their relative extent, in both systems is interesting, since it could be argued that their formation is intimately connected with the production, or otherwise, of aromatic products. It is possible that nanotubes could be the carbonaceous source of C_2H_4 and C_6H_6 as proposed by Xu and co-workers [11]. However, the absence of such products in the case of the Pd based catalyst where the concentration of nanotubes and gas-phase hydrogen is much higher than for MoO_3/H-ZSM-5 systems suggests otherwise. Alternatively, nanotube formation could arise from secondary dehydrogenation of aromatic products [25] and could therefore be enhanced in the presence of a catalyst component with a strong dehydrogenation function, such as Pd. Whether the most successful strategy to the development of optimum dehydroaromatisation catalysts is via the enhancement of activity of relatively weakly dehydrogenating catalyst components or via the partial poisoning of strongly dehydrogenating catalyst components such as Pd, remains to be seen.

4. Conclusions

In agreement with previous literature, TGA of the post-reaction carbonaceous species in methane dehydroaromatisation catalysts evidence the presence of at least two different types of cabonaceous species. Comparison of this data with that produced by the inclusion of two known promoter dopants, Ga^{3+} and Fe^{3+}, demonstrates that promotion of activity in each of these systems cannot be simply related to a general effect on carbonaceous species. The former dopant has been observed to suppress the deposition of carbon over catalysts, particularly species which are removed by higher temperature air treatment. Conversely, the latter dopant enhances the deposition of carbon, particularly species which are removed by higher temperature air treatment, although a shift in the peak maximum to lower temperatures is observed. TEM investigation of post-reaction MoO_3/H-ZSM-5 and Fe^{3+}–MoO_3/H-ZSM-5 shows that the deposition of carbon is in-homogeneous within samples and that some of the deposited carbon comprises multi-walled carbon nanotubes which grow out from the external surfaces of

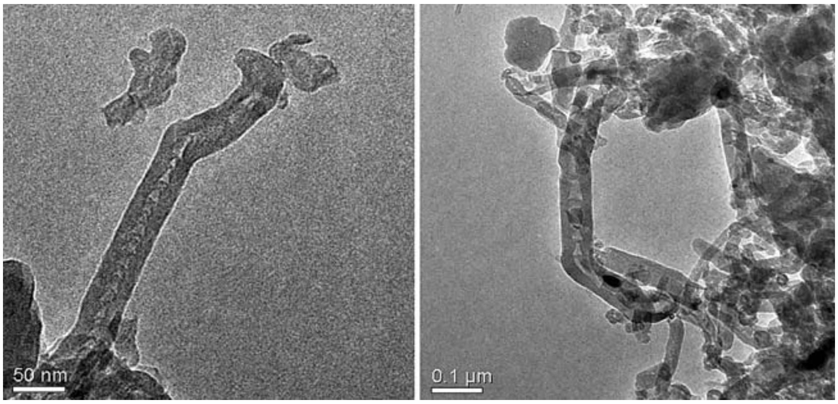

Figure 6. TEM of post-reaction 3 wt% Pd/H-ZSM-5 showing the high density of carbon nanotubes and a herring bone structured nanotube.

the ZSM-5 via a base growth type mechanism. Although many of the nanotubes are kinked, there is no evidence of the formation of herring-bone type structures. The activities of MoO_3/ZSM-5 and Pd/H-ZSM-5 for methane activation at 700 °C have been compared and it is evident that no hydrocarbon formation occurs over the latter catalyst with methane being directly cracked to yield C and H_2. TEM evidences the extensive formation of enclosed carbon nanotubes with herring-bone type structures being frequently observed. Again a base growth type mechanism for nanotube growth is proposed. It is suggested that a possible route to the necessary enhancement of currently reported methane dehydroaromatisation activities may lie in the selective poisoning of strongly dehydrogenating catalytic systems such as Pd/H-ZSM-5 rather than the enhancement of activity of relatively weakly dehydrogenating systems such as MoO_3/H-ZSM-5. The absence of accompanying hydrocarbon products in the case of the Pd based catalyst argues against the possibility of nanotubes being the source of hydrocarbons.

Acknowledgments

JSJH and SB acknowledge the EPSRC and University of Glasgow for the provision of a DTA studentship to SB. The kind assistance of Mrs. Kim Wilson in performing CHN analyses is gratefully acknowledged.

References

[1] T.R. Choudhary, E. Aksoylu and D.W. Goodman, Catal. Rev. Sci. Eng. 45 (2003) 151.
[2] Y. Xu, X. Bao and Y. Lin, J. Catal. 216 (2003) 386.
[3] F. Solymosi, J. Cserenyi, A. Szoke, T. Bansagi and A. Ozko, J. Catal. 165 (1997) 150.
[4] J.-Z. Zhang, M.A. Long and R.F. Howe, Catal. Today 44 (1998) 293.
[5] W. Li, D. Meitzner, R.L. Borry III and E. Iglesia, J. Catal. 191 (2000) 373.
[6] D. Wang, J.H. Lunsford and M.P. Rosynek, J. Catal. 169 (1997) 347.
[7] P. Meriaudeau, V.T.T. Ha and L.V. Tiep, Catal. Lett. 64 (2000) 49.
[8] S. Liu, Q. Dong, R. Ohnishi and M. Ichikawa, Chem. Commun. (1997) 1455.
[9] Y. Shu, R. Ohnishi and M. Ichikawa, J. Catal. 206 (2002) 134.
[10] R. Ohnishi, S. Liu, Q. Dong, L. Wang and M. Ichikawa, J. Catal. 182 (1999) 92.
[11] H. Liu, L. Su, H. Wang, W. Shen, X. Bao and Y. Xu, Appl. Catal. A: Gen. 236 (2002) 263and references therein.
[12] S. Qi and B. Yang, Catal. Today 98 (2004) 639.
[13] B.M. Weckhuysen, M.P. Rosynek and J.H. Lunsford, Catal. Lett. 52 (1998) 31.
[14] H. Jiang, L. Wang, W. Cui and Y. Xu, Catal. Lett. 57 (1999) 95.
[15] H. Liu, T. Li, B. Tian and Y. Xu, Appl. Catal. A: Gen. 213 (2001) 103.
[16] B.M. Weckhuysen, D. Wang, M.P. Rosynek and J.H. Lunsford, Angew. Chem. Int. Ed. Engl. 36 (1997) 2374.
[17] S. Burns, J.S.J. Hargreaves, P. Pal, K.M. Parida and S. Parija, Catal. Today 114 (2006) 383.
[18] S. Burns, J.S.J. Hargreaves, P. Pal, K.M. Parida and S. Parija, J. Mol. Catal. A: Chem. 245 (2006) 141.
[19] B. Liu, Y. Yang and A. Sayari, Appl. Catal. A: Gen. 214 (2001) 95.
[20] X. Zhu, K. Yu, J. Li, Y.-P. Zhang, Q. Xia and C.-J. Liu, React. Kinet. Catal. Lett. 87 (2005) 93.
[21] R. Levy and M. Boudart, Science 181 (1973) 547.
[22] S.T. Oyama and G.L. Haller, Catalysis, Spec. Per. Rep., Vol. 5 (RSC, Cambridge, 1982) 333.
[23] T.V. Choudhary and D.W. Goodman, Catalysis, Vol. 19 (RSC, Cambridge, 2006) 164.
[24] Y. Zhao, Y.-X. Pan, L. Cui and C.-J. Liu, Diamond Rel. Mater. 16 (2007) 279.
[25] M. Shao, Q. Li, J. Wu, B. Xie, S. Zhang and Y. Qian, Carbon 40 (2000) 2961.